Generic rigidity percolation in two dimensions

D. J. Jacobs and M. F. Thorpe
Department of Physics and Astronomy and Center for Fundamental Materials Research, Michigan State University, East Lansing, Michigan 48824
(Received 18 October 1995)

We study rigidity percolation for random central-force networks on the bond- and site-diluted generic triangular lattice. Here, each site location is randomly displaced from the perfect lattice, removing any special symmetries. Using the *pebble game* algorithm, the total number of floppy modes are counted exactly, and exhibit a cusp singularity in the second derivative at the transition from a rigid to a floppy structure. The critical thresholds for bond and site dilution are found to be 0.66020 ± 0.0003 and 0.69755 ± 0.0003, respectively. The network is decomposed into unique rigid clusters, and we apply the usual percolation scaling theory. From finite size scaling, we find that the generic rigidity percolation transition is second order, but in a different universality class from connectivity percolation, with the exponents $\alpha=-0.48\pm0.05$, $\beta=0.175\pm0.02$, and $\nu=1.21\pm0.06$. The fractal dimension of the spanning rigid clusters and the spanning stressed regions at the critical threshold are found to be $d_f=1.86\pm0.02$ and $d_{BB}=1.80\pm0.03$, respectively.

PACS number(s): 05.70.Fh, 61.43.Bn, 46.30.Cn

I. INTRODUCTION

The simple yet powerful concepts of percolation theory have found their way into many different areas of research [1,2], including communications, biology, physics, geophysics, and a host of engineering disciplines. Two important applications that commonly come to mind are those of fluid flow through porous media and the dc conductivity in a metal-insulator composite. The one essential property common to all percolation-type problems is that of a *connected pathway*. Some properties of interest, such as fluid flow or electrical current, can be traced across various paths within the system. We will apply percolation theory to random elastic central-force networks to gain insight on the geometrical aspects of elasticity where the property of interest is *rigidity*.

The elastic properties of random networks of Hooke springs has been studied over the past 12 years [3–13]. One of the most interesting findings has been that effective medium theory describes the behavior of the elastic constants and the number of floppy modes remarkably well [14,15], except very close to the phase transition from a *rigid* to a *floppy* structure. The success of effective medium theory has allowed complex situations, such as the elastic behavior of $3d$ glasses like $Ge_xAs_ySe_{1-y}$ to be characterized. In particular, some properties of glasses track the mean coordination [3,16] $\langle r\rangle=4x+3y+2(1-x-y)=2+2x+y$, where the Ge atoms are all fourfold coordinated, the As atoms are all threefold coordinated, and the Se atoms are all twofold coordinated.

Unfortunately, attempts to study the critical behavior in central-force networks have not been very satisfactory and the question of the universality class of the rigidity transition [7,8,10,12,13] has remained unresolved. This question is fundamental in understanding the nature of the rigidity transition, and may have important implications as to how the character of the glass transition is affected by the mean coordination, as has been discussed recently via *fragile* and *strong* glass formers [17]. We show here how substantial progress can be made in understanding the geometrical nature of *generic rigidity percolation* [18].

There are two important differences between rigidity and connectivity percolation. The first difference is that rigidity percolation is a vector (not a scalar) problem, and secondly, there is an inherent *long range* aspect to rigidity percolation. For example, Fig. 1(a) shows four distinct rigid clusters consisting of two rigid bodies attached together by two rods connecting at pivot joints. Now the placement of one additional rod, as shown in Fig. 1(b), *locks* the previous four clusters into a single rigid cluster [19]. This nonlocal character allows a single rod (or bond) on one end of the network

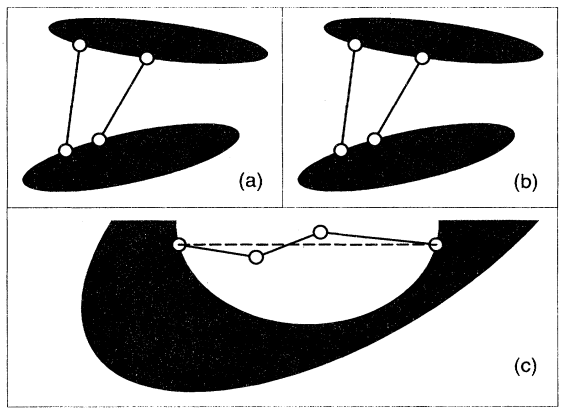

FIG. 1. The shaded regions represent $2d$ rigid bodies. The (closed, open) circles denote pivot joints that are members of (one, more than one) rigid body. (a) A floppy piece of network with four distinct rigid clusters. (b) Three generic cross links between two rigid bodies make the whole structure rigid. If the bonds were parallel, the structure would not be rigid to shear [19]. (c) Three *noncollinear* connected rods connecting across a rigid body is generic and contains one internal floppy mode. If they were collinear (along the dotted line), then there would be two *infinitesimal* (not finite) floppy motions, and under a horizontal compression buckling would occur.

to affect the rigidity *all across* the network from one side to the other.

Using concepts from graph theory, we set up *generic networks* where the connectivity or topology is uniquely defined but the bond lengths and bond angles are arbitrary. A generic network does not contain any *geometric singularities* [9] that occur when certain geometries lead to null projections of reaction forces. Null projections are caused by special symmetries, such as the presence of parallel bonds or connected collinear bonds. Rather than these *atypical* cases their generic counterparts will be present as shown in Figs. 1(b) and 1(c). This ensures that all infinitesimal floppy motions carry over to finite motions [9,20].

All previous studies on rigidity percolation have been on regular (nongeneric) lattices, which as we now know [18] have inadvertently delayed a proper understanding of the rigidity transition. In nongeneric (referred to as atypical) networks many geometrical singularities occur that lead to nonlinear effects. For example, a *diodelike* problem frequently occurs in *atypical networks* where a string of collinear bonds can only be extended with a cost in energy but can be compressed with no cost in energy due to buckling [e.g., Fig. 1(c)]. The diode effect complicates studies because it leads to the breakdown of linear elasticity theory, which must be reversible. A simple way to view a generic network is to take a regular lattice structure and randomly displace each site location by a small amount. This introduces local distortions throughout the lattice and is in itself a good physical model for amorphous and glassy materials. All prior studies that inevitably involve the nonlinear effects arising from geometrical singularities [4–14] should be considered as a separate problem.

By considering generic networks, the diode effect and the problematic geometric singularities are completely eliminated. Therefore, the problem of rigidity percolation on *generic networks* leads to many conceptual advantages because all geometrical properties are robust, not depending on a multitude of special cases. Moreover, real glasses are modeled better by generic networks rather than regular *atypical networks* because of local distortions. In two dimensions, there exist efficient, exact, combinatorial algorithms allowing for the possibility of an in-depth study of rigidity percolation.

In Sec. II, we briefly review some previous results on rigidity percolation, highlighting both the successes and the unresolved problems. We then give a short description of the *pebble game* algorithm in Sec. III, which allows the static or geometric properties of rigidity percolation in $2d$ generic networks to be addressed directly. Here we will discuss three basic applications, which include calculating the exact number of floppy modes, identifying all rigid clusters, and determining the overconstrained regions. We present results obtained using this approach in Sec. IV for the bond and site diluted generic triangular lattice. Finally, we will conclude in Sec. V with a discussion on what we have achieved in this work, and what directions still remain for further study.

II. PREVIOUS RESULTS

The rigidity of a network glass is related to how amenable the glass is to continuous deformations that require very little cost in energy. A small energy cost will always arise from weak forces that are present in addition to the hard covalent forces that involve bond lengths and bond angles. These small energies can be ignored because the degree to which the network is deformable is well quantified by just the *number* of floppy modes [3] within the system. A mental picture of floppy and rigid regions within the network has led to the idea of rigidity percolation [3,4]. An interesting model to consider is one with only central forces because its properties are most different from connectivity percolation, which can be recovered if all pivot joints are welded fixed [21,22].

Much understanding of the general phenomena of central-force rigidity percolation can be obtained by studying a random network of Hooke springs. To be specific, we begin by considering a network of Hooke springs characterized by the potential

$$V=\frac{1}{2}\sum_{\langle ij\rangle}\alpha_{ij}n_{ij}(l_{ij}-l_{ij}^{0})^{2}, \tag{1}$$

where the sum is over all bonds $\langle ij\rangle$ connecting sites i and j in the network. A bond connecting sites i and j is present if $n_{ij}=1$ with probability p and absent if $n_{ij}=0$ with probability $1-p$. The spring constants $\{\alpha_{ij}\}$ and the equilibrium bond lengths $\{l_{ij}^{0}\}$ are positive real numbers but are left arbitrary. In addition, the site locations are also left arbitrary as the network is generic. Note that *rigidity* is a static concept, involving virtual displacements, so that while it is convenient to use harmonic potentials as done in Eq. (1) any set of pair potentials would give the same results for the geometric aspects of rigidity that is of interest here.

A collection of sites form a rigid cluster when no relative motion within that cluster can be achieved without a cost in energy. Conversely, the floppy modes correspond to *finite* motions of the sample that do not cost energy. Therefore, the geometrical properties and the number of floppy modes can be determined by an equivalent bar and joint structure [9]. Note that a d-dimensional system always has at least $d(d+1)/2$ floppy modes due to d global translations and $(d-1)d/2$ global rotations.

The number of floppy modes in d dimensions is given by the total number of degrees of freedom for N sites minus the number of *independent* constraints. A redundant bond can only add additional reinforcement and/or cause internal stress in an existing rigid body. A key quantity is the number of floppy modes F in the network, or normalized per degree of freedom, $f=F/dN$. By defining the number of redundant bonds per degree of freedom as n_r, we can write quite generally

$$f=\frac{dN-[(1/2)Nzp-dNn_r]}{dN}=1-\frac{p}{p^*}+n_r, \tag{2}$$

where $p^*=2d/z$ and z is the lattice coordination. Neglecting the redundant bonds, as first done by Maxwell [23], we find that f is linear in the bond concentration p and goes to zero at the Maxwell approximation p^* for the threshold. The Maxwell approximation gives a very good account of the location of the phase transition and the number of floppy

modes, but it ultimately fails since the number of independent constraints is not just the total number of bonds, as some bonds are *dependent*.

Simple Maxwell constraint counting has been applied to $3d$ network glasses [3,11,15] with covalent bonding. Taking into account the constraints from bond stretching and bond bending forces, the number of floppy modes per degree of freedom is found to be

$$f=2-\tfrac{5}{6}\langle r\rangle, \tag{3}$$

where $\langle r\rangle$ is the average coordination number. Note that for purposes of counting the number of floppy modes and determining the rigid clusters, angular forces may be incorporated as next-neighbor central forces. Of course the quantity f cannot be negative, nor can it be zero at the rigidity threshold due to the presence of many small floppy inclusions. In the rigid phase, the approach of f toward zero as the mean coordination number increases will resemble a Lifshitz tail [24].

Short of the Maxwell constraint counting method, other ways that have been used for calculating the number of floppy modes *exactly* include rank determination of the dynamical matrix [3], relaxation methods [5,7], transfer matrix methods [6,22], Gaussian elimination [12], and the equation of motion technique [15]. Hence, many numerical methods have been explored.

Here we focus on the geometrical aspects of rigidity percolation, which have not been directly addressed before to our knowledge. Previous studies have used costly relaxation-type methods [which use $O(N^3)$ floating point operations] so that networks containing $N\approx 10^4$ sites already present a difficult numerical challenge. Relaxation methods are well suited for calculating elastic constants, but not for characterizing the geometric structure. This is because numerically one cannot identify which bond has *exactly zero* stress or if a bond *accidentally* has zero stress. However, until now, this was the only approach available in determining the stress carrying backbone.

Many basic questions have remained open regarding the nature of the rigidity transition in spite of many years of research by many groups. We mention a few points regarding the triangular lattice. Hansen and Roux [7] and later supported by Arbabi and Sahimi [12] have indicated that the fractal dimension of the stress carrying backbone is about $D_0\approx 1.63$, which is very close to the current carrying backbone in connectivity percolation. Furthermore, the elastic moduli critical exponent (also denoted by f), or more precisely the ratio $f/\nu\approx 2.95$, was obtained for the random bond-dilution problem. Curiously, this value is the same as the full bond-bending model (all angular forces are present), which has an identical geometry to connectivity percolation. These two results gave strong evidence that the geometrical properties of central-force *rigidity percolation* are identical to connectivity percolation.

At first, the idea that the two types of percolation problems could share the same universality class is surprising since the vector and scalar character have different symmetry properties and because rigidity is a highly nonlocal phenomenon much different from connectivity. However, Hansen and Roux [7] have argued that the reason this is possible is because at large length scales, the central forces are able to yield effective angular forces via *lever arms*. Thus, the central-force problem *may* renormalize into the full bond-bending model. Knackstedt and Sahimi [10] have suggested using a real space renormalization group calculation; the geometrical properties of site and bond *rigidity percolation* share the same universality class as far as geometry is concerned. However, the elastic moduli exponents were shown not to be the same. This has been confirmed by simulation [12] as well; namely, it has been found that $f/\nu\approx 1.12$ for random site dilution. If the idea of *lever arms* is correct, it should apply equally to random site dilution.

To make matters worse, other researchers [5,8] have obtained contradicting numerical results from those quoted above. One reason for all the uncertainty is the fact that only small systems were studied. This is an especially bad situation because rigidity is an inherently long range phenomenon, thus causing strong finite size corrections [7,12,25] that must be accounted for. Recently, it has been suggested [13] within mean field and a simple triangularization scheme that the rigidity transition is first order. More recently it has been shown [26] that on various Bethe lattices the rigidity transition is first order. Clearly, progress can be made if exact calculations on large system sizes become possible.

III. THE PEBBLE GAME ALGORITHM

A discussion of the pebble game algorithm in detail is out of the scope of this paper [27], but a brief description is given here. We have been able to study networks containing more than 10^6 sites, using an integer algorithm that gives exact and unique answers to the geometric properties of generic rigidity percolation. Because of the nonlocal characteristic of rigidity percolation [e.g., Figs. 1(a) and 1(b)] burning-type algorithms [2,28] commonly used in connectivity percolation are useless. This implies that the entire structure needs to be specified [29] (stored in memory) since the rigidity of a given region may depend on bonds far away.

A very efficient combinatorial algorithm, as suggested by Hendrickson [20], has been implemented to (i) calculate the number of floppy modes, (ii) locate over-constrained regions, and (iii) identify all rigid clusters for $2d$ generic bar-joint networks. The crux of the algorithm is based on a theorem by Laman [30] from graph theory.

Theorem: A generic network in two dimensions with N sites and B bonds (defining a graph) does not have a redundant bond if no subset of the network containing n sites and b bonds (defining a subgraph) violates $b\leqslant 2n-3$.

By simple constraint counting it can be seen that there must be a redundant bond when Laman's condition is violated. This necessary part generalizes to all dimensions such that if $b>dn-d(d+1)/2$ there is a redundant bond for $n\geqslant d$. For $n<d$ it follows that if $b>n(n-1)/2$ there is a redundant bond. Note that $n=1$ is an excluded case in Laman's theorem since two sites are required for a bond to be present. The essence of Laman's theorem is that in two dimensions finding $b>2n-3$ is the *only* way redundant bonds can arise. This sufficient part does not generalize to higher dimensions [20].

The basic structure of the algorithm is to apply Laman's theorem recursively by building the network up one bond at

a time. Only the *topology* of the network is specified, not the *geometry*. Because of the recursion, only the subgraphs that contain the newly added bond need to be checked. If each of these subgraphs satisfies the Laman condition, $b \leq 2n-3$, then the last bond placed is independent; otherwise it is redundant. By counting the number of redundant bonds, the exact number of floppy modes is determined.

Searching over the subgraphs is accomplished by constructing a *pebble game*. Each site in the network has two pebbles *tethered* to it. A pebble is either *free* when it is on a site or *anchored* when it is covering a bond. A free pebble represents a single motion that a site can undertake. Consider a single site having two free pebbles, representing two translations. If two additional free pebbles can be found at a different site, then the distance between this pair of sites is not fixed. Placing a bond between this pair of sites will constrain their distance of separation. To record this constraint, one of the four free pebbles is anchored to the bond. Once the bond is covered, only three free pebbles can be shared between that pair of sites. After a bond is determined to be independent, it will always remain independent and covered.

We begin with a network of N isolated sites each having two free pebbles. The system will always have $2N$ pebbles; initially two free pebbles per site. We place one bond at a time in the network connecting pairs of sites. The topological placement of either the sites or bonds will depend on the model under study such as the site- or bond-diluted generic triangular lattice as done here. The independent bonds must be covered by a pebble; therefore, before a bond can be covered it must be tested for independence. For each bond placed in the network, four pebbles (two on each site at the ends of the bond) must be free for the bond to be independent. When a bond is determined to be independent, any one of the four pebbles can be anchored to that bond. In general, all four pebbles across an added bond will not be free because they are already anchored to other bonds. These anchored pebbles may possibly become free at the expense of anchoring a neighboring free pebble while keeping a particular independent bond covered. In other words, pebbles may be shuffled around the network provided all independent bonds remain covered.

It is always possible to free up three pebbles across a bond, since they correspond to its rigid body motion. When a fourth pebble across a bond *cannot* be found, then that bond is *redundant* and it is not covered. In Fig. 2 an example of how pebbles are shuffled is shown schematically on a small generic structure. Two distinct pebbles are associated with each site for which each pebble can either be used to cover a bond or is *free* to cover a bond. The two pebbles closest to a given site as drawn schematically in Fig. 2 are the pebbles that are tethered to that site. Thus a pebble may either be on a site (free pebble) or on a bond (anchored pebble) but it always remains tethered to a given site regardless of how the pebbles are shuffled. Note that a bond may be covered by a pebble from either of its end sites. Therefore, free pebbles can be moved across the network by exchanging the site from which a pebble is used to cover a bond.

Overconstrained regions are recorded each time a dependent bond is found. These regions correspond to the set of bonds that were searched in trying to free the fourth pebble but failed. These regions, called *Laman subgraphs*, violate

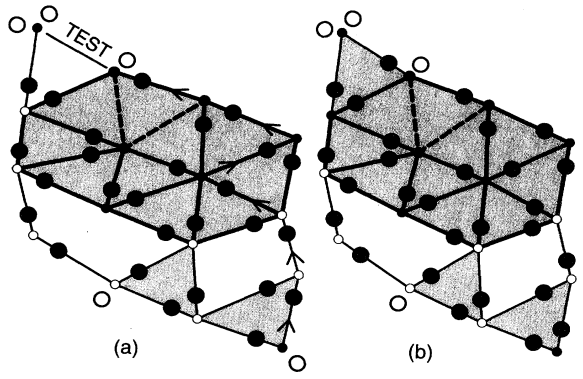

FIG. 2. A demonstration of the *pebble game* on a generic network. Independent (redundant) bonds are shown with solid (dashed) lines that are (are not) covered by a pebble. Large (filled, open) circles denote (anchored, free) pebbles on (bonds, sites). The two closest pebbles to a given site are tethered to that site. Small (filled, open) circles denote sites belonging to (one, more than one) rigid cluster. Overconstrained bonds are shown with heavy dark lines. Shaded regions denote $2d$ rigid bodies. (a) Five free pebbles indicate five floppy modes until a new bond is added and tested for independence. A fourth free pebble is found via the path traced by arrows. (b) The added bond is independent and thus covered. There are now six rigid clusters and four floppy modes.

the condition $b \leq 2n-3$. An added bond onto a Laman subgraph will be redundant.

We identify all the rigid clusters *after* the network is completely built. First, we identify isolated sites. Then the rigidity of all other sites is tested with respect to a reference bond. If a test bond between either one of the pair of sites forming the reference bond and the site in question is found to be dependent (independent) then that site is (is not) rigid with respect to the reference bond. The test bond is actually never added to the network. Since a bond can only belong to one cluster (unlike sites), all the bonds within a rigid cluster are ascribed to a particular reference bond. A systematic search is made to map out *all* rigid clusters.

We show in Fig. 2(b) the end result of the pebble game applied to a simple structure. Many aspects of rigidity are displayed. The following can be seen: (1) The exact number of floppy modes is determined by the number of free pebbles remaining. A depletion or excess of pebbles to cover a set of bonds distinguishes the overconstrained regions from the floppy regions, unlike the approximate global counting of Maxwell. (2) This network is uniquely decomposed into a set of six distinct rigid clusters, although the clusters are not disconnected. (3) The free pebble along the bottom edge cannot be shuffled over to the rigid body at the top, which already has three free pebbles. This free pebble is shared among three bars and two triangles. Generally, free pebbles get trapped in floppy regions consisting of many rigid clusters giving rise to complex collective floppy motion. (4) The number of redundant bonds is unique, whereas their locations are not unique since this depends on the order of placing the bonds. Nevertheless, each redundant bond belongs to a unique overconstrained region (Laman subgraph). For example, there are 19 overconstrained bonds in the rigid cluster at the top of the structure in Fig. 2(b), while having only two

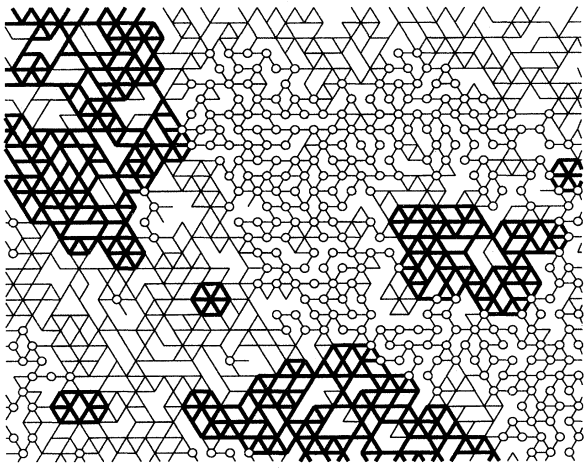

FIG. 3. The topology of a typical cutout region from a bond-diluted generic network at $p=0.6603$. A particular realization would have local distortions (not shown) similar to Fig. 2. The heavy dark lines correspond to overconstrained regions. The open circles correspond to sites that are acting as pivots between two or more rigid bodies.

redundant bonds. (5) A rigid cluster will generally have subregions that are overconstrained. If any bond that is overconstrained is removed, the rigidity of the network is unchanged.

An upper bound on the performance of the above algorithm [20] has been shown to scale according to the square in the number of sites in the system. In the implementation of the *pebble game* near the threshold, the CPU time scales roughly as $\sim N^{1.2}$, where N is the number of sites. Away from the threshold, the system size dependence is linear in N. We find that the *pebble game* runs about twice as fast for site dilution than bond dilution at their respective thresholds. Near full concentration, the performance for both the site- and bond-diluted lattices converge to the same time dependence. The difference in performance time is mainly due to a smaller effective system size for a site-diluted lattice ($N=qL^2$ instead of L^2, where q is the site concentration and L is the linear system size). On average it takes ≈ 1.4 CPU minutes on a Dec-alpha work station to find the percolating rigid cluster for a 1150×1150 bond-diluted system at its critical threshold.

A section of a large network on the bond-diluted generic triangular lattice at p_{cen} is shown in Fig. 3 after the pebble game was applied. Here we see a typical topology and associated geometry of the set of rigid clusters in this section of network. Observe that nearly all individual rigid clusters form connected paths via *pivots*, which are free joints shared by two or more rigid bodies. It can be seen that floppy regions form where the *pivot sites* cluster. Notice that within this section of the network, there is a spanning rigid cluster where *rigidity* forms a connected path from top to bottom and left to right. There are also clusters of overconstrained regions in the network that are not percolating in this section. Contrast these overconstrained regions in this figure to a typical stressed backbone shown in Fig. 1 found by Hansen and Roux (1989) [7]. Two important differences underlying the structural characteristics are that we have used generic (not atypical) networks and periodic boundary conditions in both directions (no applied rigid bus bars).

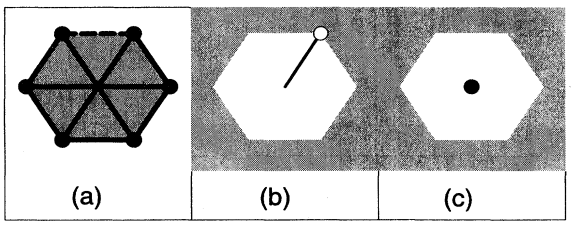

FIG. 4. All shaded areas represent a $2d$ rigid region. We show the *topology* for (a) the lowest order diagram on a triangular network to have a dependent bond (dashed line). All 12 bonds are overconstrained. (b) The lowest order diagram for a floppy inclusion corresponds to a dangling bond. (c) An isolated site is counted as a floppy inclusion and contributes two floppy modes at the next lowest order.

IV. NEW RESULTS FOR BOND AND SITE PERCOLATION

In this section, we present some new results for central-force *generic rigidity percolation* on both the bond- and site-diluted triangular net. We begin by working out a better estimate for the bond and site rigidity threshold. The Maxwell counting prediction for the site rigidity threshold gives $q^*=2/3$, which is the same as $p^*=2/3$ for bond dilution. This comes about because the number of sites in a site-diluted system is only qL^2 and the number of bonds is $q^2zL^2/2$. When the number of floppy modes is normalized per degree of freedom, the final result for f can be expressed in the same way as the left-most side of Eq. (2) with p replaced by q. To get a more accurate estimate for the rigidity threshold, the presence of redundant bonds and floppy inclusions must be accounted for.

In a low concentration expansion the first diagram to contribute redundant bonds is shown in Fig. 4(a), where only 11 of the 12 bonds are independent. This diagram leads to a correction for the number of floppy modes as $n_r = (1/2)\,p^{12}+O(p^{18})$ and $n_r=(1/2)\,q^7+O(q^{10})$ for bond and site dilution, respectively. In a high concentration expansion, the first two dominant contributing diagrams are shown in Figs. 4(b) and 4(c) corresponding to dangling ends and isolated sites. These two diagrams lead to $f=3(1-p)^5-2(1-p)^6+O((1-p)^8)$ and $f=3(1-q)^5-5(1-q)^6+2(1-q)^7+O((1-q)^8)$ for bond and site dilution, respectively.

It is these types of corrections that will shift the transition from the Maxwell threshold of 2/3 and be responsible for a non-mean-field-like critical behavior. We *equate* the number of floppy modes from the truncated low and high concentration expansions. For bond and site dilution we estimate the thresholds to be 0.6622 and 0.6877, respectively. Thus we find a small downward shift for bond dilution, and a somewhat larger upward shift for site dilution. The *pebble game* reveals that the rigidity thresholds shift about 50% more than the above estimates to $p_{cen}=0.66020\pm 0.0003$ and $q_{cen}=0.69755\pm 0.0003$ for bond and site dilution, respectively. The site-diluted threshold is also in good agreement with that obtained by Moukarzel and Duxbury [31].

It is interesting to note a couple of relationships between

floppy modes and the geometry of rigidity percolation. There is a general sum rule for f in terms of the rigid clusters in two dimensions that can be written as

$$f(p)=1-\frac{1}{2}\sum_{s=2}^{N} n_s(p)(2s-3), \tag{4}$$

where n_s is the number of rigid clusters with s sites per lattice site. Unlike connectivity percolation $\Sigma_{s=1}^{N} s n_s(p) \geq 1$ because sites are shared at pivots [e.g., Figs. 2 and 3]. If we restrict ourselves to random bond dilution, the first derivative of the floppy modes can be expressed in terms of the number of overconstrained bonds N_O as

$$f^{(1)}(p)=-\frac{z}{4}\left(1-\frac{N_O}{N_B}\right) \text{ for bond dilution,} \tag{5}$$

where N_B is the total number of bonds and z is the lattice coordination. This result can be derived by considering all possible outcomes of randomly removing *one* bond from the network. Observe that the removal of an over-constrained bond does not change the number of floppy modes whereas all other bonds increase the number of floppy modes by one.

The behavior of the number of floppy modes can be studied with great precision for bond dilution by making use of Eqs. (4) and (5). Although there is no simple formula for the second derivative, $f^{(2)}$, in terms of a geometrical quantity, it can be calculated easily with arbitrary accuracy. We only need to consider the change in the number of overconstrained bonds in the network due to the random placement of one additional bond. If all possible bond placements are considered, then $f^{(2)}$ can be calculated exactly for any given network. However, we have found that it is sufficient to perform a Monte Carlo sampling of about 5% of those bonds for a given network.

For site dilution, there is no simple expression for the first derivative of the number of floppy modes in terms of a geometrical quantity. This is because when a single site is removed, more than one bond is generally removed locally, and these bonds influence the network in a *correlated* way. However, we have calculated $f^{(1)}$ in the site-dilution case using Monte Carlo sampling by monitoring the change in the number of floppy modes caused by the random placement of one additional site. Furthermore, we also performed a Monte Carlo sampling of the random placement of pairs of sites in the network to calculate $f^{(2)}$. This latter calculation turned out to be prohibitive in calculation time for large systems.

We find that the basic characteristics of the number of floppy modes were similar for bond and site dilution. Since we obtained very accurate results for the bond-dilution case, we present these results by showing f, $f^{(1)}$, and $f^{(2)}$ in Figs. 5, 6, and 7, respectively. The results obtained for $f^{(2)}$ from our Monte Carlo sampling were found to be more accurate than a direct numerical differentiation of $f^{(1)}$. An additional benefit in calculating $f^{(2)}$ directly is that the results are independent of those for $f^{(1)}$.

A sharp peak in Fig. 7 appears without any signs of a discontinuity. The peak most resembles a simple cusp. As can be seen in Figs. 5, 6, and 7 there is virtually no difference between the data for linear system sizes $L=680$, 960, and 1150. Only very slight system size dependence has been

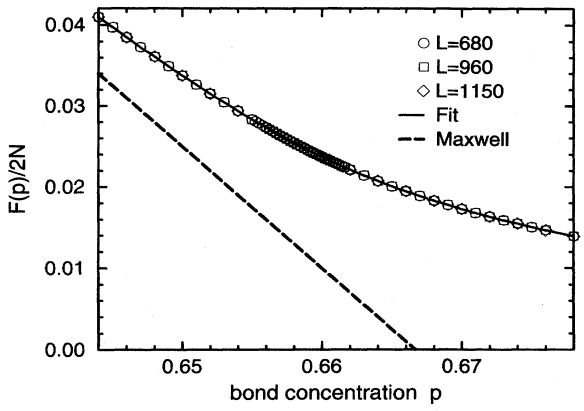

FIG. 5. Simulation results for the fraction of floppy modes, $f=F/2N$, for a bond-diluted generic network compared to the Maxwell prediction. All error bars are smaller than the symbols. Note that the nongeneric threshold [12] is at 0.641.

observed. The trend is for smaller systems to show a cusplike singularity in $f^{(2)}$ as well, but with the peak slightly shifted to the left with a smaller amplitude.

The Maxwell prediction for f is included in Fig. 5 for comparison. On this scale, the failure of the mean field estimate is evident. Nevertheless, on a scale over the range $(0 \leq p \leq 1)$ it is clear that the rigidity transition is extremely sharp and quite near the mean field threshold of 2/3. Since it is possible to obtain accurate results near the transition, both the threshold and cusp exponent can be found. The cusp singularity in $f^{(2)}$ was fitted to the functional form

$$f^{(2)}(p)=A+\Gamma_{\pm}|p-p_{cen}|^{-\alpha} \text{ for } p \gtrless p_{cen}\,. \tag{6}$$

By integrating Eq. (6) twice, both $f^{(1)}$ and f (being *independently calculated* data sets) were fitted simultaneously. Other than integration constants, no additional parameters representing analytical background terms were used in the fitting forms for $f^{(1)}$ and f. From the simultaneous fit of f, $f^{(1)}$, and $f^{(2)}$, we found an exponent of $\alpha=-0.48\pm0.05$ and a transition threshold of 0.6603 ± 0.0003. The resulting three fits

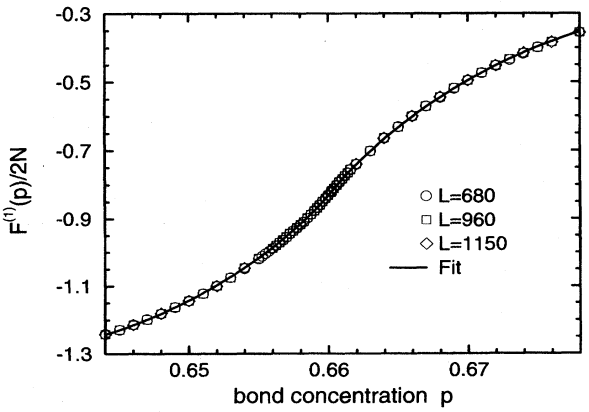

FIG. 6. The first derivative of the fraction of floppy modes for a bond-diluted generic network as calculated exactly from Eq. (5). All error bars are smaller than the symbols.

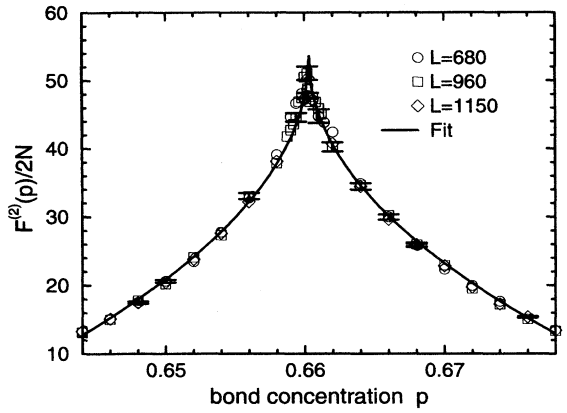

FIG. 7. The second derivative of the fraction of floppy modes for a bond-diluted generic network as calculated from Monte Carlo sampling. The fitting results for the cusp yields $p_{cen}=0.6603\pm0.0003$ and an exponent of 0.48 ± 0.05. Typical error bars are shown that reflect both the statistical errors in the Monte Carlo sampling and the ensemble averaging.

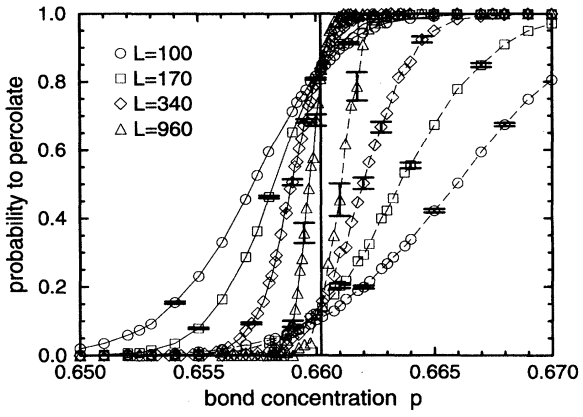

FIG. 8. The probability for a bond-diluted generic network to percolate rigidity, $P_A(p,L)$, is plotted for periodic (free) boundary conditions for various system sizes with solid (dashed) line segments drawn between data points. Only four different sizes and several typical error bars are shown for clarity. The vertical solid line indicates our extrapolated threshold.

have also been plotted in Figs. 5, 6, and 7. The fitting was over the bond concentration range shown in the figures.

The behavior of the second derivative suggests that the number of floppy modes is analogous for rigidity and connectivity percolation. In the case of connectivity percolation, the number of floppy modes is simply equal to the total number of clusters, which corresponds to the free energy [32]. It would be nice if a similar result holds for rigidity percolation. We find that the second derivative of the total number of clusters changes sign across the transition, thus violating convexity requirements. In view of Eq. (4) and that typically clusters are *not disconnected*, we suggest that the number of floppy modes generalizes as an appropriate free energy. Therefore, we have treated the exponent α in Eq. (6) in the usual context of a "heat capacity" critical exponent. More work needs to be done to see how a free energy can be defined for rigidity percolation.

We now turn to an analysis of the rigid cluster statistics, presenting results for bond dilution with free and periodic boundary conditions and site dilution with periodic boundary conditions. Since the free boundary condition data were generated mainly to check boundary effects, it was not extensively collected in comparison. Finite size scaling techniques from percolation theory [2,33] are applied assuming only a single relevant length scale exists.

We also look at the geometrical properties of the overconstrained regions motivated by our discussions with Duxbury [31]. The overconstrained regions are *not necessary* to sustain rigidity. An *isostatic framework* [9], for example, has just the right positioning of bonds to form a rigid cluster without a redundant constraint. However, when external forces are applied to a rigid isostatic framework, using rigid bus bars for example, overconstrained regions will be *induced* across it, which forms a percolating stressed region. Within a random environment there will be redundant bonds scattered throughout the network. Here the redundant bonds are essentially acting as external forces on an underlying isostatic framework. Physically, the resulting overconstrained regions characterize internal stress caused by bond mismatch. Thus, the overconstrained regions propagate stress (without externally applied forces), and are most closely analogous to the current carrying backbone in connectivity percolation. We find that monitoring the probability for a network of linear size L to contain either a spanning rigid cluster or spanning stressed backbone, leads to the same correlation length exponent ν and critical threshold.

We have looked at a series of linear system sizes ranging from $L=25$ to 1150 in increments such that the next largest size is roughly a factor of $\sqrt{2}$ larger. Our networks contain $N=L^2$ (qL^2) sites for bond (site) dilution. We typically consider about 40–50 different bond (or site) concentrations per system size. A predetermined number of bonds (or sites) are randomly placed into the system in order to have an exact concentration. For linear system sizes of $L=\{25, 35, 50, 70\}$ we have generated $N_R=10\,000$ independent realizations per concentration. For sizes $L=\{100, 120, 170, 240, 340, 480, 680, 960\}$ we have generated at least $N_R\times L^2=10^8$ number of realizations per concentration and often as much as 8 times that much. The large number of realizations were required to obtain accurate results for the probability for the system to percolate at a fixed concentration.

In Fig. 8 we plot the probability for the system to percolate, $P_A(p)$, for bond dilution with free and periodic boundary conditions. At each fixed bond concentration, we generated N_R *independent* realizations and calculate

$$P_A(p)=[N_{HV}+\tfrac{1}{2}(N_H+N_V)]/N_R. \tag{7}$$

Here N_{HV} is the number of realizations that had a spanning rigid cluster across the system both horizontally *and* vertically, whereas N_H and N_V correspond to the number of realizations that had a spanning rigid cluster only horizontally or only vertically, respectively. Other combinations of N_{HV}, N_H, and N_V were also considered following the techniques of Yonezawa, Sakamoto, and Hori [33]. We see that the prob-

ability to percolate in Fig. 8 is quite a skewed function to either side of the threshold. For large system sizes, it is expected that a fixed point will appear where all the curves cross at p_{cen}. We do see this fixed point settling down for system sizes $L \geq 100$ (more so with periodic boundary conditions). The crossing point, $P_A(p_{cen})$, is at approximately 0.85 and 0.15 for periodic and free boundary conditions, respectively, which indicates strong dependence on the boundary condition.

Various moments can be calculated from the probability density, $(d/dp)P_A(p)$, for the system to percolate. The correlation length exponent ν can then be determined accurately [2,33] from the finite size scaling of the mean width Δ_A, where

$$\Delta_A = \sqrt{\langle p^2 \rangle - \langle p \rangle^2} \sim L^{-1/\nu}. \tag{8}$$

The advantage of tracking the mean width is that it does not depend on *a priori* knowledge of p_{cen}. The critical threshold is then extrapolated using the first moment and the value of ν ascertained. We have calculated the moments according to

$$\langle p^n \rangle = 1 - n \int_0^1 x^{n-1} P_A(x) dx \tag{9}$$

by performing an integration by parts. The moments were insensitive to the method of interpolating P_A, which included joining pairs of data points by line segments, a spline fit, and fitting to suitable smooth functional forms.

The above discussion about the probability to percolate and its moments equally applies to the site dilution case. Since we expect the static critical exponents to be the *same* for bond and site dilution, as supported by a simple renormalization group calculation [10], we perform an extrapolation for ν for five different data sets as shown in Fig. 9. One data set corresponds to the percolation of rigidity for bond dilution with free boundary conditions, and the other four data sets correspond to the percolation of both rigidity and stress for bond and site dilution with periodic boundary conditions. Each extrapolated curve in the figure shows the result from five simultaneous fits of the data to the form

$$\frac{\log_{10}[\Delta_A(L)]}{\log_{10}(L)} = y = [a + \log_{10}(1 + b/L^c)] \frac{1}{\log_{10}(L)} - \frac{1}{\nu}, \tag{10}$$

where the desired exponent ν and the effective correction to the scaling exponent, c, were restricted to be the same fitting parameter for each data set. Note that if $b=0$ in Eq. (10), then one recovers a simple power law dependence with a constant amplitude given by 10^a. We find that $\nu = 1.21$ and $c \approx 0.6$ gives the best fit. We also fixed $c=1$ so that the finite size correction term would be $1/L$, which has appeared in previous extrapolations [25] for dynamical exponents. The $1/L$ correction allowed us to fit all our data nearly as well. Fixing different fitting parameters while accepting only relatively good simultaneous fits, as well as taking into account results from individual fits for each data set separately, has led us to our error estimate. We find the estimate $\nu = 1.21 \pm 0.06$.

We show in Fig. 10 the extrapolation of the critical threshold for bond dilution using three different data sets for both free and periodic boundary conditions. These results are obtained from the distributions P_I, P_A, and P_U corresponding to the intersection, average, and union of the horizontal and vertical spanning clusters [33], respectively. We have defined P_A in Eq. (7) in terms of N_H, N_V, N_{HV}, and N_R. Similarly, it follows that $P_I = (N_{HV} + N_H + N_V)/N_R$ and $P_U = N_{HV}/N_R$. Each extrapolated curve shown in Fig. 10 is

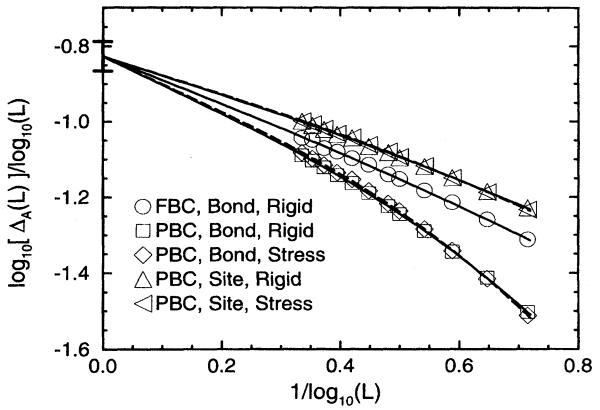

FIG. 9. An extrapolation for the exponent ν [as $1/\log_{10}(L) \to 0$] given by the inverse of the negative of the y intercept. An accurate estimate is made with five data sets simultaneously fitted to Eq. (10). Error bars are approximately the size of the symbols. The solid (dashed) lines denote the extrapolated best fit (with $\nu = 1.21$ and $c = 0.59$) for $\Delta_A(L)$ corresponding to spanning rigid (stressed) regions. The error bar at the extrapolated best value takes into account other comparatively good extrapolations. Note that the fluctuations in finding a network to percolate rigidity and stress are nearly the same.

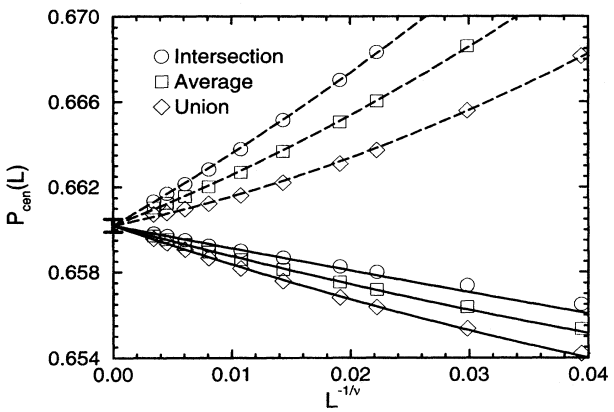

FIG. 10. The extrapolation of the rigidity threshold for bond dilution as $L^{-1/\nu} \to 0$. The different symbols represent data from three separate calculations using the distributions P_I, P_A, and P_U defined in the text. The symbol sizes reflect typical error bars. The dashed and solid lines show the best-fit curves to the data with free and periodic boundary conditions, respectively. Here we have fixed $\nu = 1.21$ and show the results from simultaneously fitting all six data sets to the form given by Eq. (11) where we find $p_{cen} = 0.6602$ and $c = 0.733$. The error bar at the extrapolated value takes into account other comparatively good extrapolations.

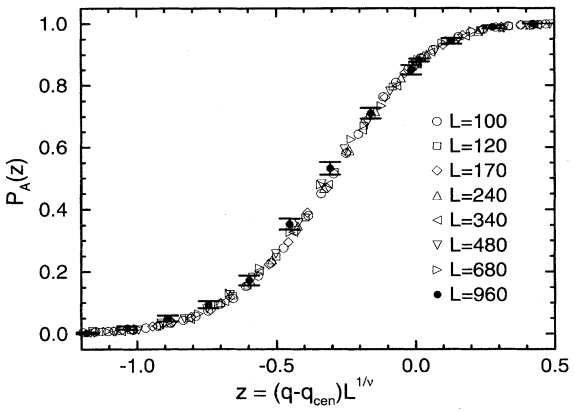

FIG. 11. The probability for a site-diluted system with periodic boundaries to percolate rigidity, $P_A(q,L)$, is plotted against the scaled axis $z=(q-q_{cen})L^{1/\nu}$ with $q_{cen}=0.69755$ and $\nu=1.21$. We note that when using the same value of the threshold, the best data collapse is obtained with a ν of 1.25, and that a good data collapse can be found with ν in the range between 1.22 and 1.28. Error bars are shown for system size $L=960$. Generally the error bars are the biggest when $P_A\approx 0.5$ for any size L, and increase as L increases because fewer realizations are generated. Also see Fig. 8, which has the same trend.

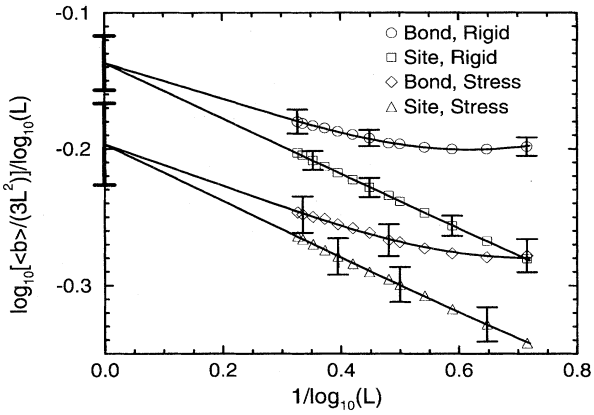

FIG. 12. The extrapolation of the fractal dimension and backbone dimension. The average number of bonds in a spanning cluster $\langle b\rangle$ is determined at the rigidity threshold for both bond and site dilution. The spanning *rigid* and *stressed* regions lead to d_f and d_{BB}, respectively. Only three typical error bars are shown on each data set for clarity.

the result of a simultaneous fit over the six data sets to the form

$$y=p_{cen}+(a+b/L^c)L^{-1/\nu}, \tag{11}$$

where the desired threshold p_{cen} was restricted to be the same fitting parameter for each data set. Note that the fitting parameters $\{a,b,c\}$ are different from those in Eq. (10). The exponent ν may be taken as 1.21 from the extrapolation in Fig. 9.

The procedure of our extrapolation is the same as that explained for estimating ν. Our error bars were determined based on fixing various parameters in Eq. (11) (such as $c=1$) as well as changing ν, while accepting only relatively good fits. We find $p_{cen}=0.66020\pm 0.0003$, which is in excellent agreement with that obtained from the cusp singularity in $f^{(2)}(p)$ as shown in Fig. 7. Similarly, for site dilution we find $q_{cen}=0.69755\pm 0.0003$.

Finite size corrections were strongest for bond dilution in Fig. 9 for periodic boundaries and in Fig. 10 for free boundaries. For site dilution (with periodic boundaries) corrections to scaling were found to be weak in both of these extrapolations. Therefore, we plot the scaled probability to percolate rigidity in Fig. 11 for site dilution. The data collapse is reasonably good over the entire range of sizes from $L=25$ to 960, suggesting only weak finite size corrections appear in site dilution. A better data collapse is possible with a ν of 1.24 as extrapolated with a $1/L$ correction to finite size scaling, which we believe should be present as a surface correction. Unfortunately, finding the best data collapse cannot assure us of having more accurate exponents since we are not strictly in the scaling regime.

At the critical threshold, a *mass* scaling analysis of the spanning rigid and stressed backbone allows the fractal dimension d_f and the backbone dimension d_{BB} to be found. Note that previous workers [5,7,12] have estimated the backbone dimension d_{BB} (denoted in Sec. II as D_0) to be 1.64. Considering both the bond- and site-dilution cases with periodic boundary conditions, we generated $N_R=5000$ additional realizations for each system size from $L=25$ to 960 and $N_R=2500$ realizations for $L=1150$. The average number of bonds (mass) in a spanning cluster, normalized by $3L^2$, will scale as L^{d_f-2}. From this we can determine β since $d_f=d-\beta/\nu$. Likewise, for the stressed backbone, its average number of bonds normalized by $3L^2$ scales as $L^{d_{BB}-2}$.

The bond- and site-dilution data are fitted simultaneously to the mathematical form given in Eq. (10) while following the same fitting procedure used to extrapolate ν. We show in Fig. 12 the resulting extrapolations. Finite size corrections are clearly seen in the bond-dilution case. We find that $d_f=1.86\pm 0.02$ and $d_{BB}=1.80\pm 0.03$. Taking $\nu=1.21$, an estimate for β as 0.169 ± 0.03 is obtained.

An order parameter can be defined as the probability for a bond to belong to the incipient infinite rigid cluster. If the rigidity transition is second order, then the order parameter should scale (for bond dilution) according to

$$P_\infty(p,L)\sim L^{-\beta/\nu}\phi[(p-p_{cen})L^{1/\nu}], \tag{12}$$

where the scaling function must have the form $\phi(z)\sim z^\beta$ for $z>0$ in the critical region. Likewise, a similar expression holds for site dilution. In Fig. 13 we plot the appropriately scaled data for bond and site dilution with periodic boundary conditions. The two sets of data collapse onto two respective curves very well, giving us the scaling function $\phi(z)$ for each case. The data collapse for the bond and site data are very good using the exponents $\nu=1.21$ and $\beta=0.175$ and the respective thresholds $p_{cen}=0.66020$ and $q_{cen}=0.69755$. There are no signs of a discontinuity in $\phi(z)$ near $z\approx 0$ to suggest a first order transition.

The β exponent is directly found from the scaling function in Fig. 14 by taking base 10 logarithms of $\phi(z)$ and z.

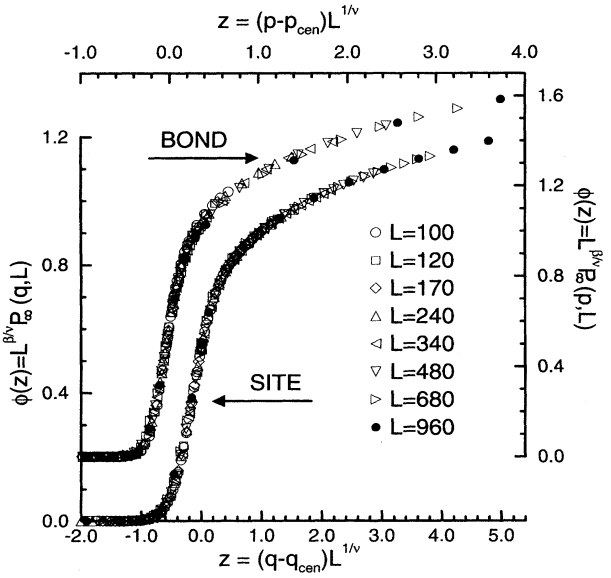

FIG. 13. The probability for a bond to be on the incipient infinite rigid cluster, P_∞, is scaled by a factor of $L^{\beta/\nu}$ for linear system sizes ranging from $L=100$ to $L=960$. We plot the scaled data, representing the scaling function $\phi(z)$, for both a bond- and site-diluted system with periodic boundaries using the top right and bottom left axes, respectively. In this plot, we used $\nu=1.21$, $\beta=0.175$, $q_{cen}=0.69755$, and $p_{cen}=0.66020$.

Fitting only the largest few system sizes over a large range in z yields a β of 0.195 and 0.170 for bond and site dilution, respectively. Some finite size effects can be eliminated by fitting the data over a restricted range (larger z) while including all system sizes from $L=100$ to $L=960$. As shown in Fig. 14, the better estimates of 0.179 and 0.171 are obtained for bond and site dilution, respectively. All four of these

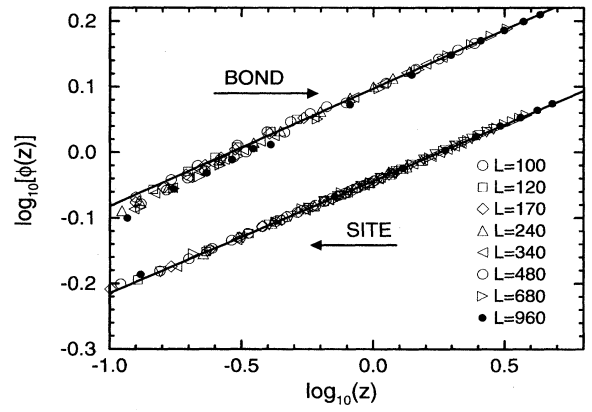

FIG. 14. Taking the data in Fig. 13, we plot the $\log_{10}$ of the scaling function $\phi(z)$ vs the $\log_{10}$ of the scaling variable z (for $z>0$) in order to estimate the β exponent from the slope of an expected straight line. We show a least squares fit (fitting over the top $\approx 50\%$ of the data points shown) that is extended through all the data points for the bond and site dilution data separately. The slopes are found to be 0.179 and 0.171 for the bond and site data, respectively.

estimates for β from the scaling function are consistent with the independent estimate of 0.169 ± 0.03 found above. Note that the site data in Fig. 14 are probably more accurate since the site data have had weaker corrections to finite size scaling on all the quantities studied. We take as our final estimate $\beta=0.175\pm0.02$ where the error bars are set by considering fits over various ranges and different system sizes.

V. DISCUSSION

We have calculated the second derivative of the number of floppy modes, $f^{(2)}$, very accurately for bond dilution. The cusp singularity in $f^{(2)}(p)$ occurs at the rigidity threshold with a cusp exponent of $\alpha=-0.48\pm0.05$ as obtained by fitting Eq. (6) to the data in Fig. 7. From the completely independent extrapolation using the probability for a bond (and site) diluted network to percolate, we found $\nu=1.21\pm0.06$. Assuming that the hyperscaling relation $\alpha=2-d\nu$ is valid, an exponent of $\nu=1.21$ suggests that the α exponent should be -0.42, which is in numerical agreement with our cusp exponent. This agreement supports our suggestion that f is the appropriate free energy density. Therefore we consider that the cusp in $f^{(2)}$ characterizes the "heat capacity" critical exponent.

Previous best estimates [7,12] for p_{cen} and q_{cen} on the regular (nongeneric) triangular network are 0.641 ± 0.001 and 0.713 ± 0.002 for bond and site dilution, respectively. The thresholds for the *generic* triangular lattice are found to be $p_{cen}=0.66020\pm0.0003$ and $q_{cen}=0.69755\pm0.0003$ for bond and site dilution, respectively. Clearly there are differences between the generic and atypical networks. Whether the critical behavior is modified is not our immediate concern, but rather our aim is to fully understand the generic case. Later it should be possible to understand the differences arising from atypical configurations containing parallel bonds, etc. Our focus will remain on generic networks since they prove easier to handle, and more importantly, they are relevant to a wide range of problems in materials science, such as amorphous materials and glasses.

We have presented extensive simulation results on central-force rigidity percolation. This has been made possible by introducing the concept of *generic* networks. Recent work by Obukhov [13] involving mean field approximations suggest that the rigidity transition is first order. It has also been shown [31] that on Bethe lattices the rigidity transition is first order. As is always the case when extrapolating simulation data, we cannot foresee unexpected trends. Thus we cannot rule out that the transition is weakly first order or even that somehow bond and site rigidity percolation are in different universality classes. However, by making the plausible assumption that the static nature of the rigidity transition is the same for site and bond dilution (as supported by our data) we are led to a very consistent picture. Namely, that the rigidity transition is second order and is in a different universality class to connectivity percolation. We summarize our results for the static critical exponents in Table I.

In conclusion, we obtained the static critical exponents by using the usual cluster moment definitions [2] except for the *specific heat* exponent α, which was estimated from $f^{(2)}$ as shown in Fig. 7. The usual definition in connectivity percolation that the total number of clusters correspond to the free

TABLE I. Summary of the static exponents for rigidity percolation, as estimated from the bond- and site-diluted generic triangular lattice. A comparison is made to connectivity percolation.

Percolation	α	β	ν	d_f	d_{BB}
Connectivity	-0.667	0.138	1.333	1.896	1.62
Rigidity	-0.48 ± 0.05	0.175 ± 0.02	1.21 ± 0.06	1.86 ± 0.02	1.80 ± 0.03

energy [32] is not suitable because convexity requirements break down. In this respect more work is needed to find an appropriate model Hamiltonian that maps to rigidity percolation. This would also give more insight into how other physical properties relate to the rigid clusters.

More generally, we have shown how the concept of a generic graph, as introduced by Laman [30] and amplified by Hendrickson [20] can greatly simplify problems concerned with the percolation of rigidity. The surprise is that networks that lack any symmetry (generic models) are easier to deal with. This concept leads to a common p_{cen} for all generic bond-diluted triangular networks and to a common q_{cen} for all generic site-diluted triangular networks. Furthermore, both models share the same static critical exponents α, β, γ, ν, etc. It remains to be seen if the exponent f that describes the elastic response is also the same for bond- and site-diluted generic networks. To explore this question, relaxation methods can be used. This too can be done more efficiently on generic networks [31] than has been done on atypical networks because the *pebble game* can be used to identify the stress carrying part of the network *before* relaxing the network.

While the *pebble game* used in this paper is only applicable in $2d$, we are currently extending the rules for the pebble game to $3d$, where the Laman condition is necessary but no longer sufficient [20,30,34]. We believe that progress can be made provided we restrict ourselves to a specific topology where it is possible to enumerate those cases where sufficiency in the Laman condition fails. This is an important step in extending this powerful technique to real covalent glasses. In the meantime, it is important to more fully understand the $2d$ case where immediate progress can be made.

ACKNOWLEDGMENTS

We thank A. R. Day, B. R. Djordjević, P. M. Duxbury, P. Leath, S. B. Lee, H. Nakanishi, and J. Tersoff for useful discussions. We are particularly indebted to B. Hendrickson for his help in explaining how Laman's theorem is relevant to this problem. This work was partially supported under NSF Grant No. CHE-92 24102. A copy of this program for analyzing $2d$ generic networks is available upon request [35].

[1] S. Kirkpatrick, Rev. Mod. Phys. **45**, 574 (1973); J. W. Essam, Rep. Prog. Phys. **43**, 843 (1980); R. Zallen, *The Physics of Amorphous Solids* (Taylor and Francis, London, 1985).
[2] D. Stauffer, *Introduction to Percolation Theory* (Taylor and Francis, London, 1985).
[3] M. F. Thorpe, J. Non-Cryst. Solids **57**, 355 (1983).
[4] S. Feng and P. Sen, Phys. Rev. Lett. **52**, 216 (1984).
[5] A. R. Day, R. R. Tremblay, and A-M. S. Tremblay, Phys. Rev. Lett. **56**, 250 (1986).
[6] S. Roux and A. Hansen, Europhys. Lett. **6**, 301 (1988).
[7] A. Hansen and S. Roux, Phys. Rev. B **40**, 749 (1989); J. Stat. Phys. **53**, 759 (1988).
[8] C. D. Hughes, C. J. Lambert, and D. Burton, J. Phys. Condens. Matter **2**, 3399 (1990).
[9] E. Guyon, S. Roux, A. Hansen, D. Bideau, J.-P. Trodec, and H. Crapo, Rep. Prog. Phys. **53**, 373 (1990).
[10] M. A. Knackstedt and M. Sahimi, J. Stat. Phys. **69**, 887 (1992).
[11] D. S. Franzblau and J. Tersoff, Phys. Rev. Lett. **68**, 2172 (1992).
[12] S. Arbabi and M. Sahimi, Phys. Rev. B **47**, 695 (1993).
[13] S. P. Obukhov, Phys. Rev. Lett. **74**, 4472 (1995).
[14] S. Feng, M. F. Thorpe, and E. J. Garboczi, Phys. Rev. B **31**, 276 (1984).
[15] H. He and M. F. Thorpe, Phys. Rev. Lett. **54**, 7355 (1985); Y. Cai and M. F. Thorpe, Phys. Rev. B **40**, 10 535 (1989).
[16] J. C. Phillips, J. Non-Cryst. Solids **34**, 153 (1979); **43**, 37 (1981).
[17] M. Tatsumisago, B. L. Halfpap, J. L. Green, S. M. Lindsay, and C. A. Angell, Phys. Rev. Lett. **64**, 1549 (1990); R. Böhmer and C. A. Angell, Phys. Rev. B **45**, 10 091 (1992).
[18] D. Jacobs and M. F. Thorpe, Phys. Rev. Lett. **75**, 4051 (1995); M. F. Thorpe, D. J. Jacobs, and B. R. Djordjević (unpublished).
[19] V. Heine (private communication).
[20] B. Hendrickson, Siam J. Comput. **21**, 65 (1992); (private communications).
[21] Y. Kantor and I. Webman, Phys. Rev. Lett. **52**, 1891 (1984).
[22] D. Bergman, Phys. Rev. B **31**, 1696 (1985).
[23] J. C. Maxwell, Philos. Mag. **27**, 294 (1864).
[24] I. M. Lifshitz, Adv. Phys. **13**, 483 (1969).
[25] J. G. Zabolitzky, D. J. Bergman, and D. Stauffer, J. Stat. Phys. **44**, 211 (1985); M. Sahimi and S. Arbabi, *ibid.* **62**, 453 (1990)
[26] C. Moukarzel, P. M. Duxbury, and P. Leath (unpublished).
[27] D. J. Jacobs and B. Hendrickson (unpublished).
[28] J. Hoshen and R. Kopelman, Phys. Rev. B **14**, 3438 (1976).
[29] The large memory requirements can be dramatically reduced by monitoring only *pivot* sites, which are shared among two or more rigid clusters. We estimate system sizes of 10^8 sites are accessible by building the network up layer upon layer. This can be done by (1) applying temporary rigid bus bar boundary

conditions, (2) removing of unnecessary storage, and (3) then removing the bus bars before adding the next layer.
[30] G. Laman, J. Eng. Math. **4**, 331 (1970).
[31] C. Moukarzel and P. M. Duxbury, Phys. Rev. Lett. **75**, 4055 (1995); P. M. Duxbury (private communication).
[32] C. M. Fortuni and P. W. Kastelyn, Physica **57**, 536 (1977).
[33] Y. Yonezawa, S. Sakamoto, and M. Hori, Phys. Rev. B **40**, 636 (1989).
[34] D. S. Franzblau, Siam J. Discuss. Math. **8**, 388 (1995).
[35] A copy of the *pebble game* program can be obtained by internet from either Jacobs@pa.msu.edu or Thorpe@pa.msu.edu.

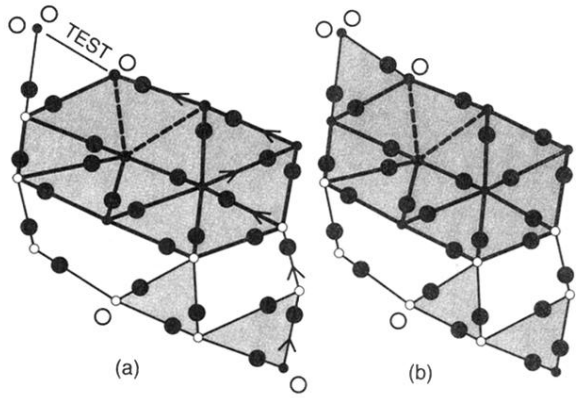

FIG. 2. A demonstration of the *pebble game* on a generic network. Independent (redundant) bonds are shown with solid (dashed) lines that are (are not) covered by a pebble. Large (filled, open) circles denote (anchored, free) pebbles on (bonds, sites). The two closest pebbles to a given site are tethered to that site. Small (filled, open) circles denote sites belonging to (one, more than one) rigid cluster. Overconstrained bonds are shown with heavy dark lines. Shaded regions denote $2d$ rigid bodies. (a) Five free pebbles indicate five floppy modes until a new bond is added and tested for independence. A fourth free pebble is found via the path traced by arrows. (b) The added bond is independent and thus covered. There are now six rigid clusters and four floppy modes.

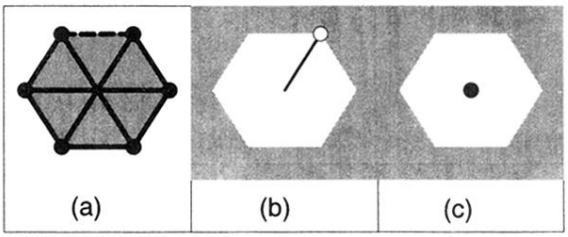

FIG. 4. All shaded areas represent a $2d$ rigid region. We show the *topology* for (a) the lowest order diagram on a triangular network to have a dependent bond (dashed line). All 12 bonds are overconstrained. (b) The lowest order diagram for a floppy inclusion corresponds to a dangling bond. (c) An isolated site is counted as a floppy inclusion and contributes two floppy modes at the next lowest order.